A Comparison of Two Banded, Heavy Snowstorms with Very Different Synoptic Settings

MICHAEL L. JUREWICZ SR. AND MICHAEL S. EVANS

NOAA/NWS Forecast Office, Binghamton, New York

(Manuscript received 9 October 2003, in final form 28 June 2004)

ABSTRACT

Two banded, heavy snowstorms that occurred over the northern mid-Atlantic region are compared and contrasted. On 6–7 January 2002, a narrow, intense band of heavy snow was observed, along with several other weaker bands, embedded within a large area of moderate snow. On 19–20 January 2002, a single, broader band of heavy snow was observed, embedded within a broken area of light snow.

The synoptic-scale settings associated with these two storms were strikingly dissimilar. In the first case, strong quasigeostrophic (QG) forcing for ascent was present just to the south of the heavy snowfall area. A highly amplified longwave trough was located over the Mississippi River valley, while a compact shortwave trough moved northward, up the east side of the longwave trough. The result was robust cyclogenesis off of the mid-Atlantic coast. In the second case, the relatively weaker QG forcing for ascent was located much farther southwest of the snowband. The flow aloft was much less amplified, with weaker cyclogenesis occurring off of the mid-Atlantic coast.

Analysis of the frontal scale environments for both cases indicated that the snowbands were each associated with the collocation of midtropospheric frontogenesis and reduced stability. In the first case, evidence is shown that a layer of potential symmetric instability (PSI) was located just above a deep, sloping zone of frontogenesis, in the presence of deep near-saturated conditions. In the second case, evidence is shown that a layer of potential instability (PI), associated with rapidly decreasing relative humidity with height, was located just above a shallow, sloping zone of frontogenesis. In addition, it is shown that a particularly favorable thermal environment for snowflake growth and accumulation became collocated with the heavy snowband. It is hypothesized that the differences in the intensity and horizontal extent of the bands observed with these two events resulted from differing atmospheric responses associated with the areal extent of large-scale and frontogenetical forcing, moisture availability, degree of instability, and specific thermal profiles.

1. Introduction

Numerous studies have been carried out on favorable environments for the development of intense, small-scale (widths of 5–40 km) bands of heavy snow within relatively large (100–500 km wide) regions of light to moderate stratiform snow (e.g., Martin 1998a,b; Nicosia and Grumm 1999; Schultz and Schumacher 1999; Clark et al. 2002). These types of bands typically form in regions of strong, large-scale forcing for upward motion, within the upward branch of a thermally direct circulation associated with frontogenesis. The bands associated with the frontogenesis become narrowed and intensified when decreased stability acts to localize and intensify the frontal circulation (as described by the Sawyer–Eliassen equation; Bluestein 1993). A modeling study by Thorpe and Emanuel (1985) confirmed that reduced dry symmetric stability on the warm side of a sloping frontal boundary acts to strengthen and narrow frontal circulations associated with frontogenesis.

Many other studies have examined the effect of combining an unstable atmosphere with frontogenesis. The scenario most commonly studied is when conditional symmetric instability (CSI) coincides with the upward branch of a frontogenetical circulation. CSI is defined as the condition for which a saturated atmosphere is stable to vertical and horizontal displacements, but unstable to slantwise displacements. Areas of saturation in the vicinity of frontogenesis are favorable locations for the release of CSI, because slantwise ascent, directed up a sloping frontal zone, typically occurs within the upward branch of a thermally direct frontogenetical circulation. In cases where the lift associated with frontogenesis coincides with a layer of CSI, it has been shown that very narrow, intense bands of precipitation can develop (i.e., Bennetts and Hoskins 1979; Sanders 1986; Nicosia and Grumm 1999; Wiesmueller and Zubrick 1998).

The operational diagnosis of CSI typically involves one of two commonly used techniques. One technique

Corresponding author address: Michael S. Evans, NWS Forecast Office, 32 Dawes Dr., Johnson City, NY 13790.
E-mail: michael.evans@noaa.gov

is to examine cross sections taken perpendicular to the thermal wind of saturation equivalent potential temperature (θ_{es}) and geostrophic momentum ($m_g = u_g - fy$), where u_g is the geostrophic wind component into the plane of the cross section, f is the Coriolis parameter (increasing with latitude), and y is the horizontal axis of the cross section, increasing toward the cold air. Assuming that the background flow is two-dimensional (2D) and in geostrophic balance, then CSI is present when the slope of the θ_{es} surfaces is steeper (more vertical) than the slope of the m_g surfaces (Bluestein 1993). Schultz and Schumacher (1999) demonstrated that potential symmetric instability (PSI), defined as an unstable condition for slantwise ascent, *assuming that air parcels can be lifted to saturation*, can be diagnosed by likewise comparing the slope of the equivalent potential temperature (θ_e) surfaces and m_g surfaces.

A second technique commonly used to evaluate the presence of CSI is to calculate moist potential vorticity (MPV) in a layer, where MPV $= -\vartheta_g \cdot \nabla\theta_{es}$ (Schultz and Schumacher 1999). In this equation, ϑ_g is the three-dimensional geostrophic vorticity vector, and ∇ is the three-dimensional gradient (''del'') operator. Likewise, the presence of PSI can be evaluated by calculating equivalent potential vorticity (EPV) in a layer, where EPV $= -\vartheta_g \cdot \nabla\theta_e$ (Martin et al. 1992; Moore and Lambert 1993). It can be shown that MPV (EPV) is negative in regions characterized by conditional instability (potential instability), inertial instability (the atmosphere is unstable to horizontal displacements), or CSI (PSI) (Schultz and Schumacher 1999; Moore and Lambert 1993).

Problems associated with using vertical cross sections of θ_{es} and m_g to evaluate the presence of CSI were summarized by Schultz and Schumacher (1999). For example, the assumption that the flow is 2D is often of questionable validity in cases of robust cyclogenesis; in fact, those cases are usually associated with strongly curved flow that is not 2D relative to a vertical cross section, no matter what the orientation of the cross section [i.e., the geostrophic wind is not constant in the along-front direction (into the cross section)]. In addition, the assumption that the background flow is geostrophic is also questionable in highly curved flow regimes where the ageostrophic component of the wind can be large due to the effects of the curvature. Because of the potential problems associated with examining cross sections of θ_{es} and m_g, Schultz and Schumacher (1999) recommend the use of the MPV technique for diagnosing the presence of CSI. However, it should be noted that finding areas of negative MPV does not provide information on whether the implied instability is slantwise, vertical, or inertial. A cross-sectional analysis of θ_{es} would still be useful to make that distinction.

Another issue related to the identification of CSI is whether or not the total wind can be substituted for the geostrophic wind in the calculation of MPV. This issue was also addressed by Schultz and Schumacher (1999); they recommend use of the geostrophic wind because that would be more consistent with the parcel theory associated with CSI, which assumes a geostrophic background flow. The parcel theory associated with CSI also assumes that the background environment is nonchanging on the time scale over which the slantwise convection is occurring. A similar assumption regarding the time scales of the background environment and convective processes is also made in the parcel theory associated with vertical convection; that is, the convection is assumed to occur over a small enough time scale so that the large-scale background environment does not have time to change significantly while the parcel is accelerating vertically. Gray and Thorpe (2001) argue that the assumption that the time scale of the convection is much less than the time scale of large-scale environmental changes may not be as valid for slantwise convection as it is for vertical convection. As such, it can be argued that there are times when the potential for slantwise convection can best be determined by comparing the acceleration of the parcel with the acceleration of an evolving, unbalanced environmental background. Based on this argument, it can be shown that the potential for slantwise acceleration of air parcels relative to an evolving and unbalanced environment can best be described by using MPV calculated using the total wind (J. Nielson-Gammon 2003, personal communication). Use of the total wind to calculate MPV can also sometimes be advantageous when examining diagnostics from high-resolution datasets, because the geostrophic wind fields from the high-resolution datasets can be considerably noisier than the total wind fields, making geostrophic MPV relatively noisy and difficult to interpret (Schultz and Schumacher 1999). Clark et al. (2002) demonstrated that the value of MPV can vary greatly, depending on whether vorticity (or momentum) is calculated using the geostrophic or total wind. In their case study, they found that negative MPV corresponded best to the development of snowbands when the geostrophic wind was used in the calculation. MPV and EPV, using both the geostrophic wind and the total wind, are available to operational forecasters in the National Weather Service via the Advanced Weather Interactive Processing System (AWIPS).

The large-scale conditions that favor the coincidence of CSI and frontogenesis have been examined by several previous studies. Nicosia and Grumm (1999) studied three banded snowstorms over the northern mid-Atlantic region and concluded that CSI naturally occurs in regions of midtropospheric frontogenesis associated with cyclogenesis. CSI develops as a dry midtropospheric airstream (the dry slot), associated with the midtropospheric trough, sweeps cyclonically over the top of the greatest influx of moisture in the lower troposphere. In these cases, often associated with rapid surface cyclogenesis, θ_{es} surfaces become steeper as midlevel drying results in a reduction of θ_{es} with height, while the m_g surfaces flatten as the vertical shear increases. Novak

et al. (2004) examined a large collection of cold-season-banded events associated with heavy precipitation over the eastern United States and found some key similarities in the large-scale patterns. Specifically, they found that single bands typically developed northwest of surface cyclones, in areas of strong midtropospheric deformation and frontogenesis. They also found that significant bands typically developed with systems associated with rapid cyclogenesis and deep cyclonic circulations (''closed off'' through at least 700 hPa). Martin (1998a,b) showed a Midwest case where heavy, banded convective snow developed in association with relatively modest surface cyclogenesis; however, the midtropospheric flow was still quite amplified and closed off through the midtroposphere.

The aforementioned studies indicate that bands of very heavy snow typically occur with the collocation of frontogenesis and instability, which is favored northwest of surface cyclones, in highly amplified large-scale flow patterns. However, several recent studies indicate that less intense, but still significant, snowbands can occur in other locations relative to a surface cyclone, and in other types of large-scale flow environments. Schumacher (2003) and Banacos (2003) showed cases where modest snowbands developed northeast of surface cyclones. The bands in their case studies were less intense than the bands in Novak et al. (2004), but were still able to produce some 1–2 in. (2.5–5 cm) h^{-1} accumulation rates. Skerritt et al. (2002) examined a case where snowbands developed within an area of large-scale frontogenesis, but with no nearby surface cyclone. Again, the bands in their study were less intense than in Novak et al. (2004), but still produced snowfall amounts of 5–10 in. (12.5–25 cm).

In addition to the collocation of frontogenesis and instability, another factor that should be considered when diagnosing the potential for heavy, banded snowfall is the expected snow-to-liquid ratio of the precipitation. Heavy snow is most favored in areas where thermal, moisture, vertical motion, and wind profiles are most favorable for high snow-to-liquid ratios (Wetzel and Martin 2001). Low-density snowflakes are associated with high snow-to-liquid ratios. Previous research indicates that low-density dendritic snow crystals typically develop in environments characterized by saturation, upward vertical motion, and temperatures ranging between $-12°$ and $-18°$C (Power et al. 1964). Snowflakes can become more dense when they fall through layers that contain large amounts of supercooled water, which is favored at temperatures between $-5°$ and $-10°$C (Power et al. 1964; Roebber et al. 2003). Aggregation processes (i.e., snowflakes sticking together) typically result in lower-density snowflakes and are most favored at temperatures between $0°$ and $-4°$C. Other factors that lead to low-density snowflakes and resulting high snow-to-liquid ratios include light surface winds and a cold ground (Roebber et al. 2003).

In summary, the aforementioned studies indicate that heavy, banded snowstorms typically occur in association with large-scale flow patterns that favor the development of midtropospheric frontogenesis and midtropospheric instability or weak stability, and a favorable environment for high snow-to-liquid ratios. The purpose of this study is to illustrate some of the variety of large-scale patterns that can lead to the development of these features by examining two cases of heavy, banded snowfall that appeared to be associated with dramatically different synoptic regimes. The first case, which occurred on 6–7 January 2002 was characterized by a very narrow (approximately 10 km in width), intense snowband, along with several less intense bands, embedded within a large area of moderate snow. This case was associated with strong quasigeostrophic (QG) forcing for ascent and rapid surface cyclogenesis. The second case, on 19–20 January 2002 was accompanied by a single, nearly stationary, wider (width of approximately 30 km) band of heavy snow, embedded within a larger, broken area of light snow. In contrast to the first case, the QG forcing for ascent was relatively small and located well to the southwest of the snowband, and the surface cyclogenesis was modest.

Section 2 of this paper will briefly discuss the data sources used to diagnose the two events in this study. Section 3 describes the first case and section 4 describes the second case. A discussion is presented is section 5, followed by a summary in section 6.

2. Data sources and methodology

The model data used for these two cases were data from the Eta Model stepped terrain model (Black 1994) displayed using the General Meteorological Package, version 5.6L (GEMPAK 5.6L) (desJardins et al. 1991). The data were displayed on a 40-km grid, with a vertical resolution of 25 hPa. For the first case (6–7 January), analysis grids from the 1200 UTC 6 January and 0000 UTC 7 January runs of the model were used. For the second case (19–20 January), analysis grids and forecast data through 9 h were used from the 1200 UTC 19 January run of the Eta Model.

For the calculation of the divergence of **Q** vectors, the data were thinned to an 80-km grid spacing, prior to the calculation (using the IJSKIP = 1 calculation in GEMPAK). A five-point smoother was also applied to the divergence of **Q**-vector plots. The radar data shown for the two cases are 2-km-resolution mosaics of 0.5° reflectivity data from the national Weather Surveillance Radar-1988 Doppler (WSR-88D) network. The frontogenesis calculated by GEMPAK is a two-dimensional version of the frontogenesis equation (Miller 1948) with the tilting and diabatic heating terms omitted.

3. Overview: 6 January 2002

A large area of moderate snow overspread the northern mid-Atlantic region during the afternoon on 6 Jan-

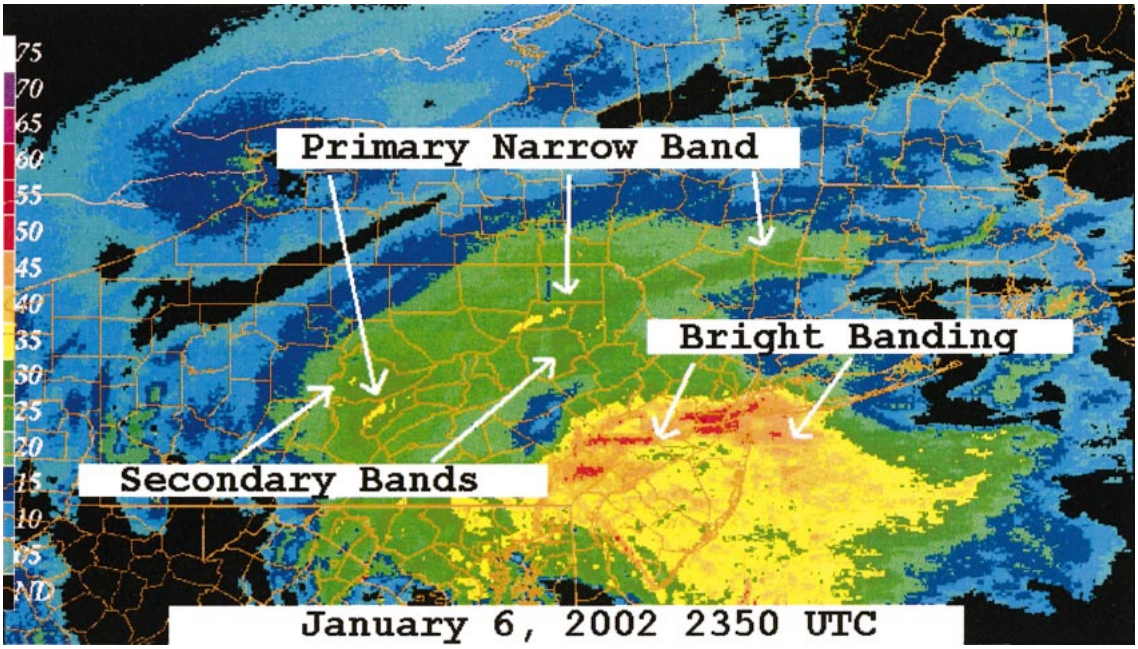

FIG. 1. A 2-km-resolution WSR-88D mosaic of 0.5° reflectivity at 2300 UTC 6 Jan 2002.

uary as a surface low pressure system developed rapidly along the mid-Atlantic coast. Narrow bands of heavy snow developed within this larger area of moderate snow by late afternoon. Figure 1 shows a 2-km-resolution WSR-88D mosaic of reflectivity at 2300 UTC on 6 January. Note the primary narrow band of heavy snow extending from eastern New York southwest to central Pennsylvania. The band was characterized by maximum reflectivity values of around 35 dBZ. The width of the band was approximately 10 km, and the length was approximately 400 km. Other shorter, less intense bands were located north and south of the main band across Pennsylvania. The higher-reflectivity values over southeast Pennsylvania and New Jersey were associated with mixed and melting precipitation (e.g., bright banding). In summary, this event appeared to correspond to the single band heavy snow events studied by Novak et al. (2004). During the late afternoon and evening on 6 January the primary intense band moved north, while the large area of moderate snow moved to the northeast. As a result, the heavy snow associated with the primary narrow band produced a wide swath (approximately 100 km wide) of 10–18-in. (approximately 25–45 cm) snow accumulations (Fig. 2). Most locations in the heavy snow area reported snowfall rates of 2–5 in. h^{-1} (5–12.5 cm h^{-1}), for a few hours while the band was passing over their location. Some localized unofficial storm totals (not shown) exceeded 20 in. (approximately 50 cm) in far northeast Pennsylvania.

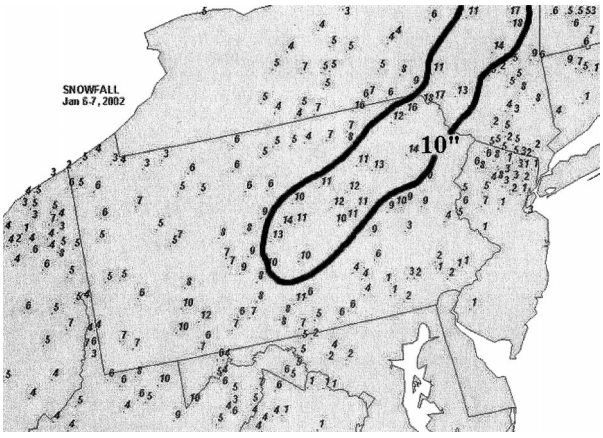

FIG. 2. Observed snowfall (in.) from 1200 UTC 6 Jan 2002 through 1200 UTC 7 Jan 2002 (from the central Pennsylvania Weather Forecast Office).

Figure 3 shows a four-panel display of Eta Model analyses of some meteorological parameters commonly utilized in the forecast process that are valid at 0000 UTC 7 January. The upper-tropospheric wind pattern at 0000 UTC 7 January indicated that Pennsylvania and New York were under the left exit region of an upper-tropospheric speed maximum located over the eastern Carolinas. At 500 hPa, a pronounced longwave trough is evident extending from the Great Lakes region south to the lower Mississippi River valley. A compact shortwave trough was lifting northeast up the eastern side of the longwave trough over North Carolina and Virginia. At 700 hPa, a closed cyclonic circulation was centered over the central Appalachian Mountains, while at the surface, a 996-hPa low pressure center was deepening along the Maryland coast. The surface low was observed to deepen approximately 8 hPa during the 6-h period from 1800 UTC 6 January through 0000 UTC

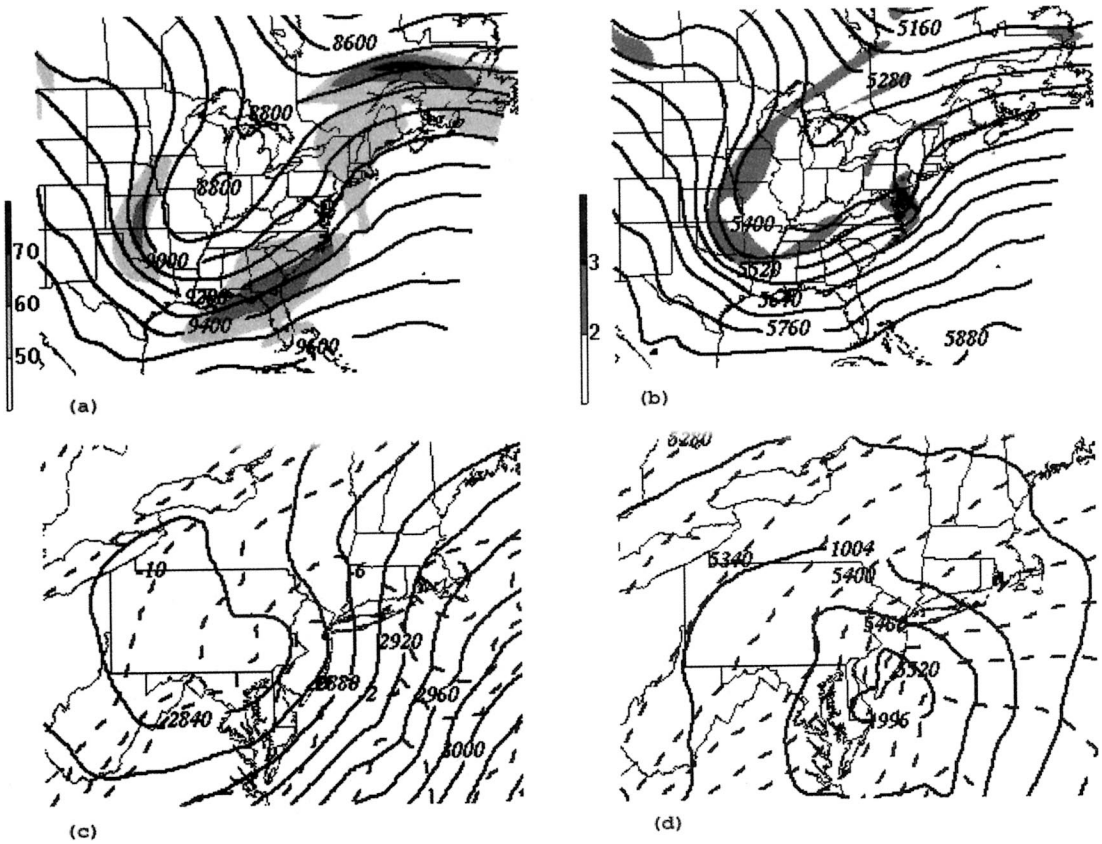

FIG. 3. Eta analysis of (a) 300-hPa geopotential height (m) and wind speed of 40 m s^{-1} or greater (shaded), (b) 500-hPa geopotential height (m) and absolute vorticity (shaded, 10^{-4} s^{-1}), (c) 700-hPa geopotential height (m) and temperature (°C), and (d) mean sea level pressure (hPa) and 1000–500-hPa thickness (m), and all valid at 0000 UTC 7 Jan 2002.

7 January. In short, this appeared to be a classic mid-Atlantic cyclogenesis event, with strong dynamic forcing resulting from a highly amplified mid- and upper-tropospheric flow pattern, a compact midtropospheric shortwave trough, and rapid lower-tropospheric cyclogenesis (Kocin and Uccellini 1990).

Strong QG forcing at 0000 UTC 7 January was indicated by the magnitude of the **Q** vector convergence shown in Fig. 4a. Figure 4a shows the Eta Model analysis of the 300–500-hPa-layer **Q**-vector divergence, where negative values imply QG forcing for large-scale lift. An elongated northwest to southeast maximum of convergence can be seen, corresponding to the midtropospheric shortwave shown in Fig. 3, centered over northern Delaware. Figure 4b shows the corresponding Eta Model analysis of 600-hPa omega. The omega field exhibits one maximum east of the Delmarva Peninsula, and a second maximum over northeast Pennsylvania. The northeast Pennsylvania maximum is stretched in a southwest-to-northeast orientation, similar to the orientation of the observed snowband.

A cross section of an Eta Model analysis of frontogenesis (using the total wind) and omega (Fig. 5) shows the mesoscale vertical structure that contributed to the formation of the band within the area of large-scale upward vertical motion forcing indicated by the **Q** vectors. The cross section is taken from Atlantic City, New Jersey (ACY), to Binghamton, New York (BGM) (across the axis of the snowband), and is valid at 0000 UTC 7 January. Note that significant frontogenesis was indicated across the axis of the snowband. Specifically, two maxima of frontogenesis are indicated; the most pronounced maxima starts at the surface near ACY and slopes upward toward the northwest reaching a level at around 800 hPa southeast of BGM, while a second starts at around 700 hPa northwest of ACY and slopes upward to just above 600 hPa southeast of BGM. The axis of maximum omega is forecast on the warm side of the frontogenesis, implying a thermally direct circulation. A maximum value of lift (between 15 and 20 μb s^{-1}), apparently associated with the snowbands over northern Pennsylvania, is evident between 600 and 500 hPa. The close relationship between frontogenesis and the model omega shown by this figure indicates the important role that frontogenesis played in focusing the upward motion in the snow area.

In this case, both the axis of maximum geostrophic 500–700-hPa frontogenesis and the maximum of 500–700-hPa **Q**-vector convergence (not shown) were located south of the maximum of the 500–700-hPa ageo-

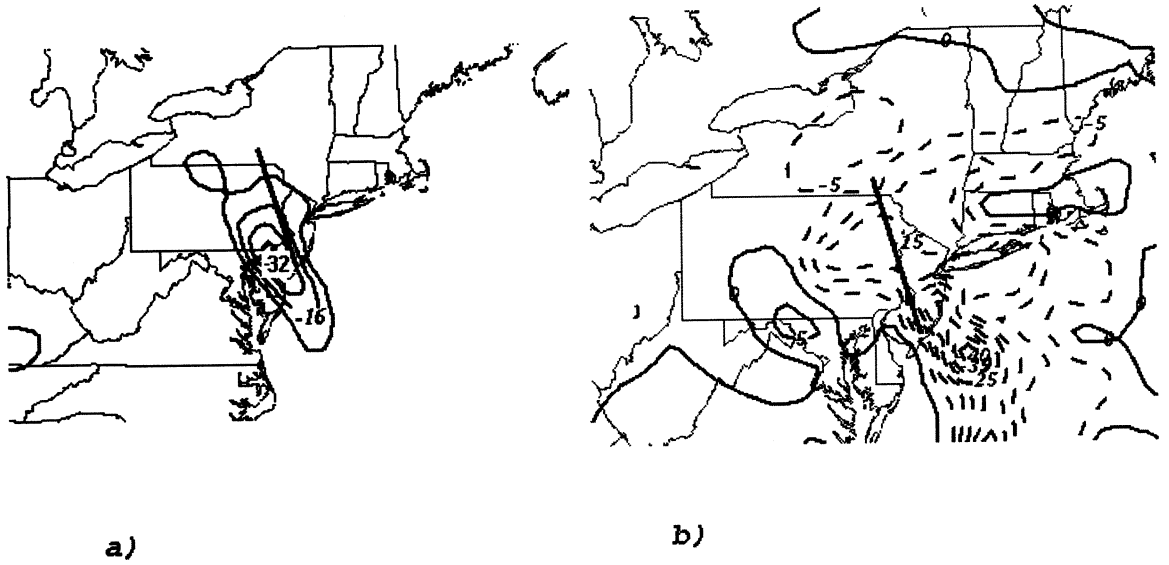

FIG. 4. Eta analysis of (a) divergence of **Q** in the layer from 500 to 300 hPa (10^{-14} K m^{-2} s^{-1}, only negative values plotted) and (b) 600-hPa omega (μb s^{-1}), both valid at 0000 UTC 7 Jan 2002. The straight line from New Jersey to southern New York indicates the location of the cross sections shown in Figs. 5 and 7.

strophic frontogenesis and omega. This indicates that the maximum forcing for upward motion, as determined by the large-scale geostrophic flow, was located south of the maximum frontal scale, ageostrophic forcing, and lift. The fact that the location and orientation of the snowband was more strongly correlated with the ageostrophic frontal scale forcing and lift again indicates the important role that the smaller-scale forcing played in producing the snowband.

As was discussed in the introduction, previous research on banded snowstorms indicates that heavy snowbands typically occur in the presence of both frontogenesis and instability (or relatively weak stability) on the warm side of the front. The most favorable configuration is one where the lift associated with the frontogenesis extends upward into the unstable (or weakly stable) zone (i.e., Nicosia and Grumm 1999). A two-panel display of Eta Model analysis data valid at 0000 UTC 7 January (Fig. 6) illustrates how well this case fits that model. The 600-hPa (total wind) frontogenesis and negative 500–600-hPa EPV (Fig. 6a) appear to be collocated, with axes extending from central Pennsylvania eastward to northern New Jersey. The axes appear to coincide fairly well with the area of moderate snow that was occurring over Pennsylvania and southeast New York around 0000 UTC 7 January. Figure 6b shows the 600-hPa heights and negative absolute geostrophic vorticity, valid at 0000 UTC 7 January. The instability, frontogenesis, and heavy snow areas all appear to be coincident with a midtropospheric shortwave ridge and a corresponding area of near-zero to slightly negative absolute geostrophic vorticity, located just downstream of the shortwave trough moving north along the east coast.

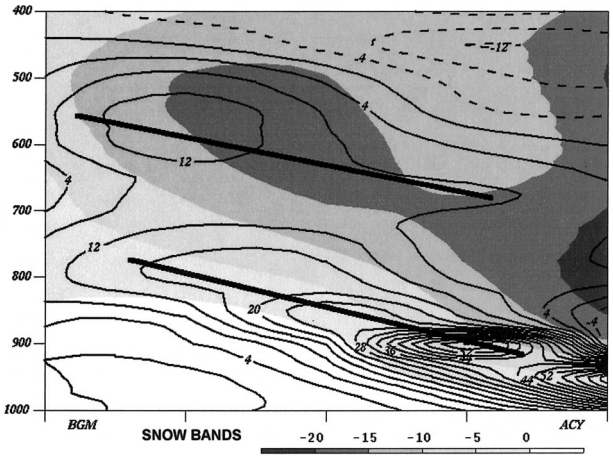

FIG. 5. Eta analysis cross section from BGM to ACY of frontogenesis [black lines, 1×10^{1} K (100 km)$^{-1}$ (3 h)$^{-1}$] and omega (shaded, μb s^{-1}) valid at 0000 UTC 7 Jan 2002. The SNOW BANDS caption marks the approximate location of the intense snowbands that occurred across northern Pennsylvania. The thick black lines indicate the two primary axes of frontogenesis.

The existence of the region of negative EPV coincident with the downstream ridge can be explained by considering the Eta Model forecast cross sections shown in Fig. 7. Figure 7a shows a 12-h Eta forecast cross section of θ_e, m_g, relative humidity, and EPV taken roughly normal to the temperature gradient, from ACY to BGM, that is valid at 0000 UTC 7 January. Note that the atmosphere was near saturation (relative humidity greater than 80%) through a deep layer in this area; therefore, any differences between θ_e and θ_{es} would be minimal. In this figure, the midtropospheric m_g surfaces are flat at 600 hPa, in the area where the intense snow-

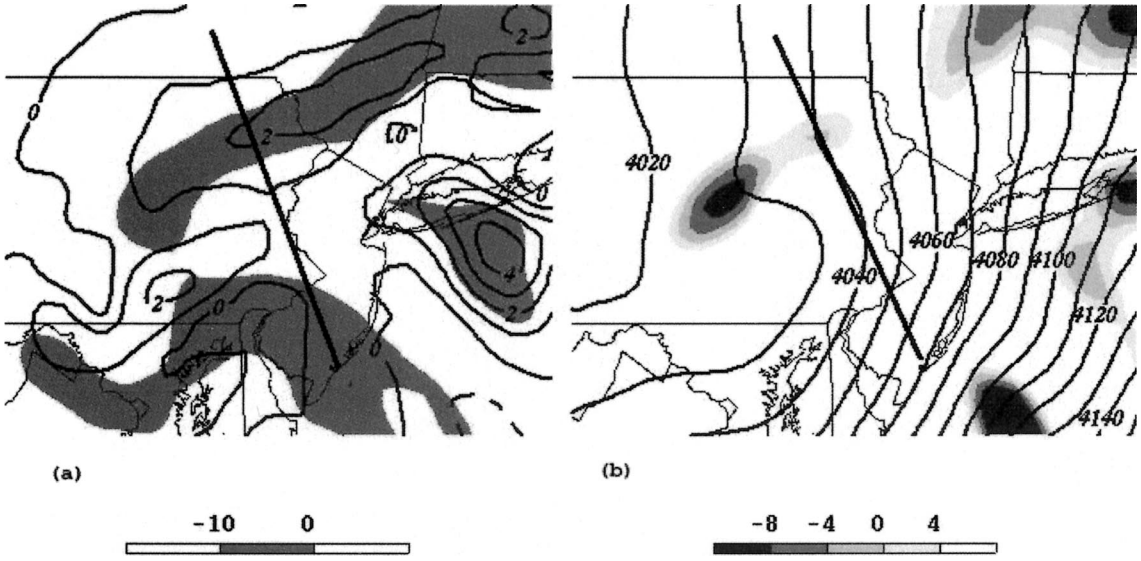

FIG. 6. Eta analysis of (a) 600-hPa frontogenesis [K (100 km)$^{-1}$ (3 h)$^{-1}$] and 600–500-hPa negative EPV [shaded, 10^{-7} K (Pa s)$^{-1}$], and (b) 600-hPa geopotential height (m) and negative absolute vorticity (shaded, 10^{-5} s^{-1}), all valid at 0000 UTC 7 Jan 2002. The straight black lines indicate the position of the cross sections shown in Figs. 5 and 7.

band was collocated with the midtropospheric ridge. Below 600 hPa, the m_g surfaces appear to slope downward toward the north. Meanwhile, the θ_e surfaces throughout this area have a very shallow upward slope, and a large area of negative EPV is indicated. The flat to downward slope of the m_g surfaces in this area indicates a rapid increase in the geostrophic wind component into the plane of the cross section with increasing latitude. This implies inertial neutrality at 600 hPa, and inertial instability in the layer below 600 hPa where the m_g surfaces slope downward. Recall that inertial instability implies that air parcels within this region would be unstable to horizontal displacements. Recall also that an inertially unstable environment is associated with negative EPV.

A cross section (the same as that shown in Fig. 7a) of θ_e, negative EPV, relative humidity, and momentum calculated using the total wind, is shown in Fig. 7b. Note the significant difference in the slope of the momentum surfaces above the location of the snowband, when the total wind is used to calculate momentum as opposed to the geostrophic wind. The momentum surfaces are now shown to slope upward toward the north in the area where the heavy snowband developed, and just a small area is indicated where the θ_e contours are slightly steeper than the (total wind) momentum con-

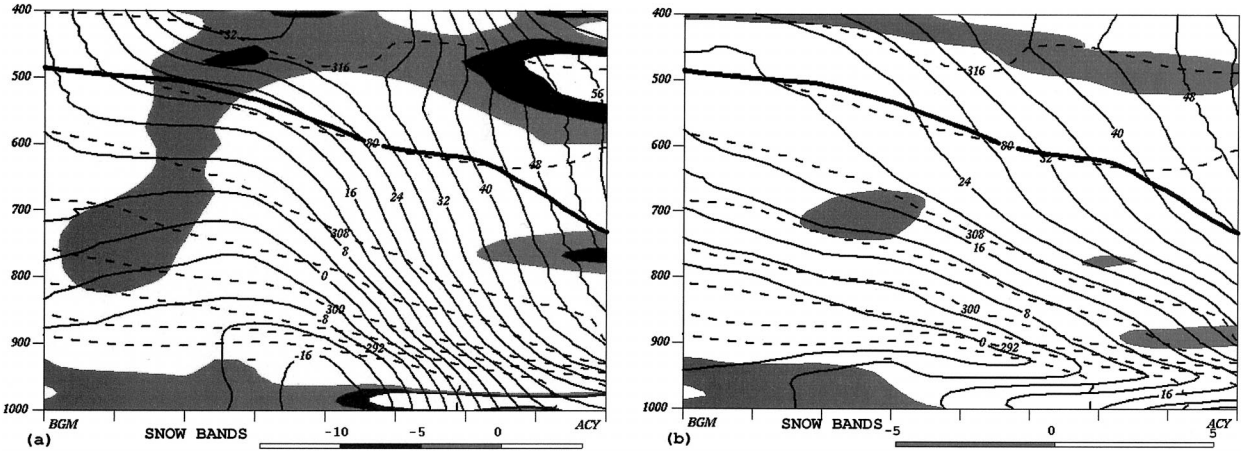

FIG. 7. Eta analysis cross sections from ACY to BGM of (a) θ_e (dashed lines, K), m_g (solid lines, m s^{-1}), relative humidity (80% value represented by the thick, solid line; all areas below the thick, solid line have relative humidities greater than 80%), and negative geostrophic EPV [shaded, 10^{-7} K (Pa s)$^{-1}$] and (b) θ_e (dashed lines, K), momentum calculated with the total wind (solid lines, m s^{-1}), relative humidity (%, same convention as in Fig. 7a), and negative EPV calculated using the total wind [shaded, 10^{-7} K (Pa s)$^{-1}$], all valid at 0000 UTC 7 Jan 2002. The SNOW BANDS caption marks the approximate location of the intense snowbands that occurred across northern Pennsylvania.

tours. A small area of negative (real wind) EPV is also indicated in that area, indicating a small area of PSI.

The fact that the momentum surfaces calculated using the geostrophic wind indicated an inertially neutral to unstable midtropospheric environment corresponding to the snowband location, while the real-wind momentum surfaces indicated a small region of PSI, begs the question: was inertial instability really a factor in producing the heavy snowbands associated with this event? Or, was the inertial instability indicated by the geostrophic wind quickly mixed out by the total wind, resulting in an atmosphere with a small area of PSI, as indicated by the data in Fig. 7b? Displaying cross-sectional data of m_g with 40-km grid spacing frequently results in apparent areas of inertial instability in the vicinity of small-scale ridges in the geopotential height field (Novak et al. 2002). While 40 km may be a small enough grid spacing to resolve these ridges, it is not small enough to resolve the very narrow convective elements indicated by Fig. 1. Therefore, the most reasonable interpretation of these data may be that the inertial stability of the atmosphere in the vicinity of the frontogenesis was weakly positive, while the potential symmetric stability was neutral to weakly negative over very small areas. The acceleration of the flow due to the inertial instability implied by the data in Fig. 7a was unlikely; however, some parcel accelerations may have occurred due to the PSI indicated in Fig. 7b.

The evolution of the environmental characteristics on 6 January related to snowflake microphysics and snow-to-liquid ratios is summarized by the data in Fig. 8. Model soundings from the analysis of the 1200 UTC 6 January and 0000 UTC 7 January runs of the Eta Model, taken at Avoca, Pennsylvania (AVP) (Fig. 8a), indicate that the sounding evolved to produce a deep surface–based layer favorable for aggregation at 0000 UTC 7 January, with a shallow layer favorable for dendrite production in the midtroposphere. The sounding appeared to cool below 800 hPa between 1200 and 0000 UTC, while slight warming occurred between 800 and 700 hPa. The combination of temperature advection, vertical motion, and diabatic cooling (evaporational cooling, and cooling due to melting implied by the onset of moderate snow around 1900 UTC) responsible for the evolution of the temperature profile is summarized in Fig. 8b. The lower-tropospheric cooling appeared to occur in combination with cold advection and diabatic cooling (the surface temperature fell 6°F in 1 h when snow began at AVP around 1900 UTC), while the midtropospheric warming seemed to be the result of warm advection in the absence of significant upward vertical motion (the strongest midtropospheric upward vertical motion occurred just after 0000 UTC). The snow-to-liquid ratios for the 24-h period ending 1200 UTC 7 January (Fig. 8c) indicate that the ratios with this event ranged from 10:1 to 15:1 (Fig. 8c), or about normal for the area.

4. Overview: 19 January 2002

An east-to-west-oriented band of snow developed near the border of New York and Pennsylvania during the early afternoon (about 1800 UTC) on 19 January. The band intensified as it remained nearly stationary for about 6 h, then pivoted toward the southeast and weakened by early evening (around 0000 UTC 20 January). Associated snowfall was most pronounced around 2100 UTC, when radar returns of 25–35 dBZ were observed across parts of southern New York (Fig. 9). The band itself had about a 30-km width, and was several hundred kilometers in length. A narrow corridor across the southern tier of New York received heavy snowfall (Fig. 10).

Large-scale forcing for ascent was not well collocated with the heavy snowband during this event. Figures 11a and 11b illustrate that an axis of enhanced midtropospheric omega over New York and Pennsylvania was better correlated with the position of the snowband than was the **Q**-vector convergence field. A maximum in **Q**-vector convergence, which extended from Ohio into West Virginia, appeared to be associated with both the right entrance region of an upper-tropospheric jet maximum over New York and the approach of a midtropospheric shortwave trough (Figs. 12, 13a, and 13b). Meanwhile, a less pronounced maximum in **Q**-vector convergence was noted over eastern New York, just east of where the main snowband developed. This implies that there could have been some weak coupling between synoptic-scale forcing in the upper troposphere, and frontal scale forcing in the midtroposphere. Overall, however, disorganized large-scale support was observed near the snowband over southern New York and northern Pennsylvania. Several other diagnostics support an initial conclusion that the greatest large-scale QG forcing would be well removed from where the heavy snowband occurred. In the midtroposphere, a zonal flow pattern was in place, with individual shortwaves propagating from west to east across the continental United States. The feature of interest was a trough moving out of the lower Mississippi River valley. Although some darkening was evident at the base of this system on water vapor imagery (Fig. 12), the midtropospheric trough axis was positively tilted and embedded within a low-amplitude flow regime (Fig. 13a). These factors suggested that the primary QG forcing would stay well south and west of the state of New York. In addition, little or no divergence was indicated at 300 hPa over the area where the heavy snowband developed, because this region was positioned almost directly underneath the core of a strong jet streak (Fig. 13b). As a result, large-scale 300-hPa divergence and induced lift typically found underneath the right entrance region were displaced toward the south and west over Kentucky, West Virginia, and the mid-Atlantic region from southern Pennsylvania into the Carolinas. At 700 hPa, a flat southwesterly flow was also indicated over the eastern United States, ahead of a relatively weak and positively

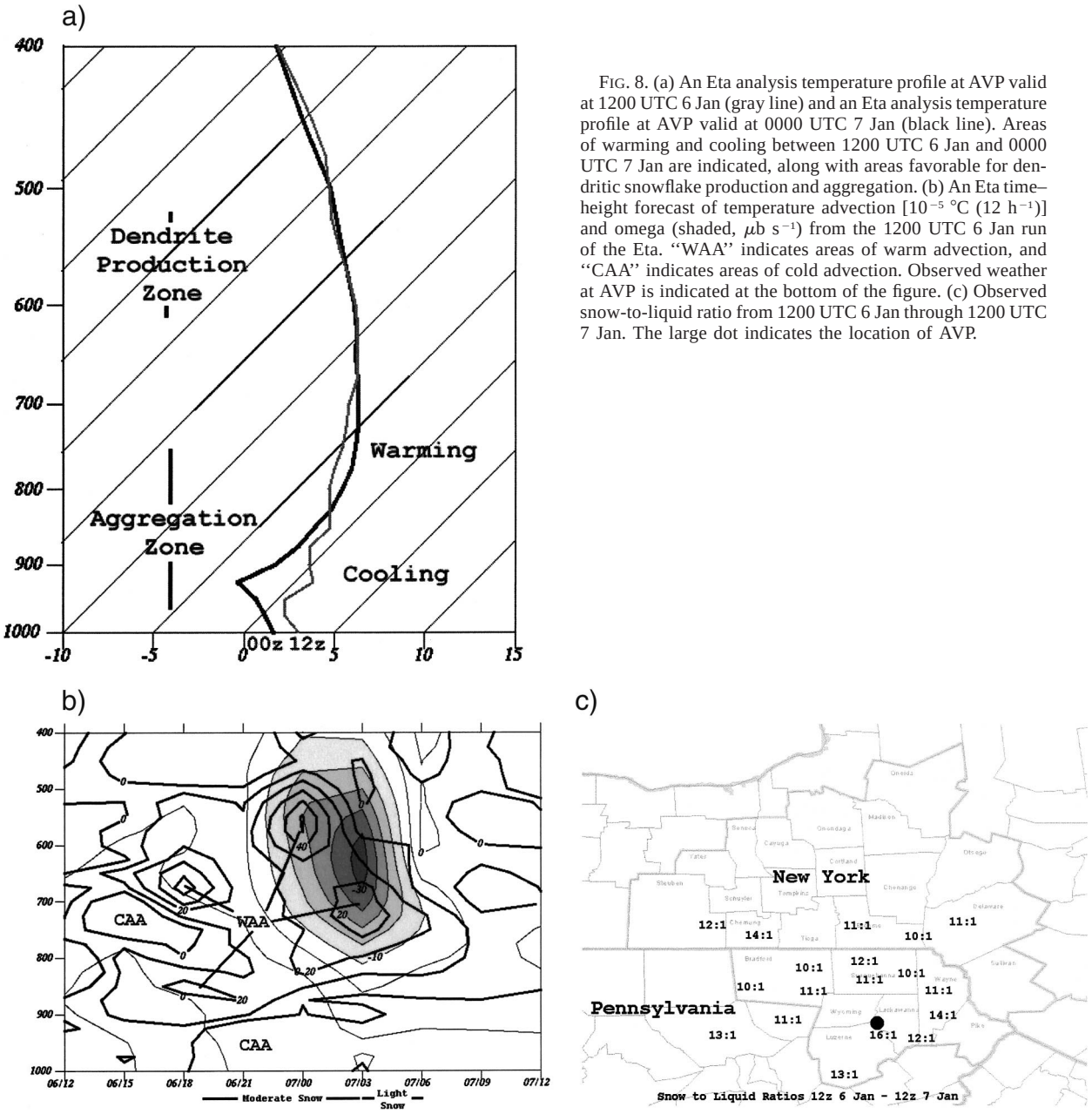

FIG. 8. (a) An Eta analysis temperature profile at AVP valid at 1200 UTC 6 Jan (gray line) and an Eta analysis temperature profile at AVP valid at 0000 UTC 7 Jan (black line). Areas of warming and cooling between 1200 UTC 6 Jan and 0000 UTC 7 Jan are indicated, along with areas favorable for dendritic snowflake production and aggregation. (b) An Eta time–height forecast of temperature advection [10^{-5} °C (12 h^{-1})] and omega (shaded, $\mu b\ s^{-1}$) from the 1200 UTC 6 Jan run of the Eta. ''WAA'' indicates areas of warm advection, and ''CAA'' indicates areas of cold advection. Observed weather at AVP is indicated at the bottom of the figure. (c) Observed snow-to-liquid ratio from 1200 UTC 6 Jan through 1200 UTC 7 Jan. The large dot indicates the location of AVP.

tilted trough axis (Fig. 13c). This was in contrast to 6 January, when the 700-hPa flow was much more amplified and displayed a closed-off circulation center (Fig. 3c).

The lower-tropospheric environment featured a weak surface wave off of the Virginia coast, with a secondary low pressure center over the southern Appalachians (Fig. 13d). The flat nature of the midtropospheric flow precluded the opportunity for either system to intensify significantly. The lack of enhanced surface development for this case represents a stark difference from many documented cases with heavy snowband formation. In such cases, the deepening rate of the surface cyclone was often at least 15 hPa in a 24-h period (Nicosia and Grumm 1999; O'Handley and Bosart 1989). The fact that the surface cyclone was not well developed contributed to a relatively weak lower-tropospheric (surface to 850-hPa layer) pressure gradient over the northeastern United States, which, in turn, limited the magnitude of the lower-tropospheric flow over New York and northern Pennsylvania. This lack of wind flow is another unusual characteristic, compared to many other heavy snowband cases. It has been well documented in previous research that the development of a lower-tropospheric jet streak [typically termed the cold conveyor belt (CCB)] is an important ingredient for both inflow

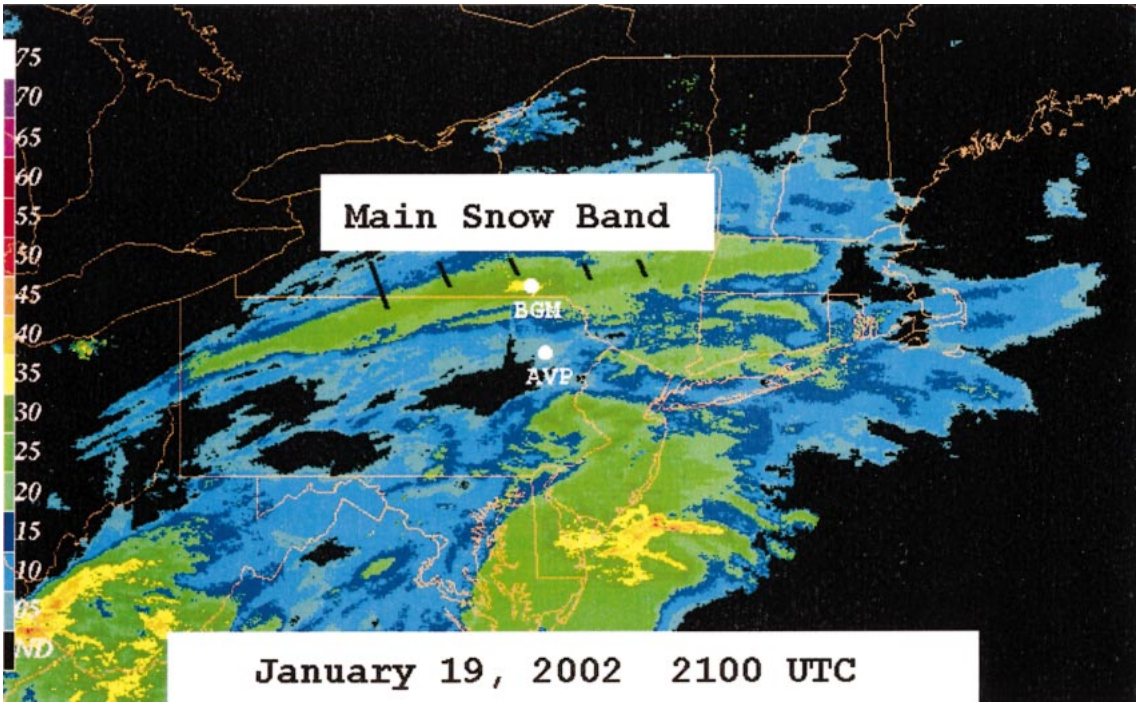

FIG. 9. A 2-km-resolution WSR-88D mosaic of 0.5° reflectivity at 2100 UTC 19 Jan 2002.

of deeper moisture and destabilization resulting from differential θ_e advection with height (Wiesmueller and Zubrick 1998; Carlson 1980).

For this case, it is theorized that while the large-scale environment may not have been favorable for the development of heavy precipitation over New York, the frontal scale environment possessed the mechanisms required for localized areas of heavy snow. An inspection of the 1200 UTC 19 January run of the Eta Model in plan view and cross-sectional formats, valid at 2100 UTC 19 January (Figs. 14a and 14b), showed an enhanced area of frontogenesis across Pennsylvania and southern New York, implying the presence of a vertically sloped frontal boundary across that area. The front extended upward from near the surface across the Delmarva region to the midtroposphere over New York. An axis of omega is indicated along and just to the warm side of the frontogenesis, with a relative maximum (around 8 μb s^{-1}), apparently associated with the snowband, evident over southern New York in the 600–500-hPa layer (Fig. 14b). It should be noted that the magnitude of the omega for this event is considerably less than what was observed on 6–7 January (15–20 μb s^{-1}). A visual comparison between Figs. 9, 10, 14a , and 14b shows good correlation in time and space between heavy snowfall over southern New York and an elevated frontogenesis maximum (just below 600 hPa). However, a similar comparison between Figs. 9, 15a, and 16a also shows much weaker radar returns across central and most of northeastern Pennsylvania were well correlated to both a relative minimum of frontogenesis and a drier, more stable midtropospheric environment seen over this area. It is theorized by the authors that this combination of less frontal forcing and more stability resulted in a weaker ageostrophic circulation, less lift, and lighter precipitation. The less intense character of the precipitation over northeastern Pennsylvania, compared to southern New York, is confirmed by the data in Table 1, which displays a comparison between the surface observations at BGM and AVP, during the afternoon and early evening period of 19 January (refer back to Fig. 9 for a geographical reference). The data on this table illustrate that the snow was much heavier and

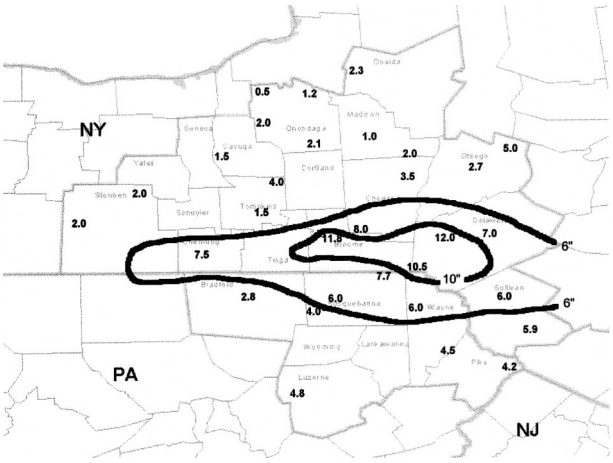

FIG. 10. Snowfall totals (in.) from 1200 UTC 19 Jan 2002 to 1200 UTC 20 Jan 2002.

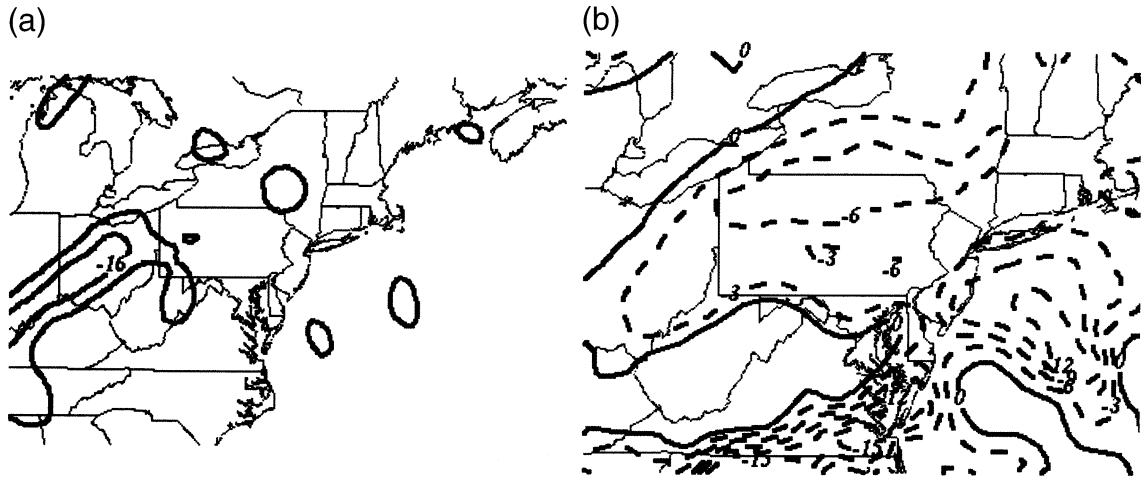

FIG. 11. Eta analysis of (a) divergence of **Q** in the layer from 500 to 300 hPa (solid, 10^{-14} K m^{-2} s^{-1}, only negative values plotted) and (b) 600-hPa omega (dashed, μb s^{-1}), both valid at 2100 UTC 19 Jan 2002.

steadier at BGM than it was at AVP. Further south, across southeastern Pennsylvania and the Delmarva region, radar coverage and echo intensity seem to increase once again, which corresponds well to more pronounced frontal scale forcing in the lower troposphere across that area.

In summary, the data from this case indicate that the band of heavy snow was collocated with midtropospheric frontogenesis, in the absence of organized large-scale forcing. A logical subsequent area to examine is whether any unstable layers existed above the frontal zone. For the 19 January case, Fig. 15a indicates that a shallow, but pronounced, unstable layer was present directly above the midtropospheric frontogenesis maximum. The data in Fig. 15b show a layer in the midtroposphere between 600 and 450 hPa where relative humidity and θ_e decrease rapidly with height, thus, implying an area of PI (Schultz and Schumacher 1999). The midtropospheric frontogenesis maximum associated with the snowband over southern New York was well collocated with this area of PI (Figs. 15a and 15b). As such, the existing frontal circulation was likely enhanced by the PI. The decrease in relative humidity with height appears to have been associated with a midtropospheric dry slot over Pennsylvania, as indicated by the forecast relative humidity pattern shown in Fig. 16a. Figure 16b portrays the differential θ_e advection associated with the dry slot, with negative θ_e advection above 550 hPa and

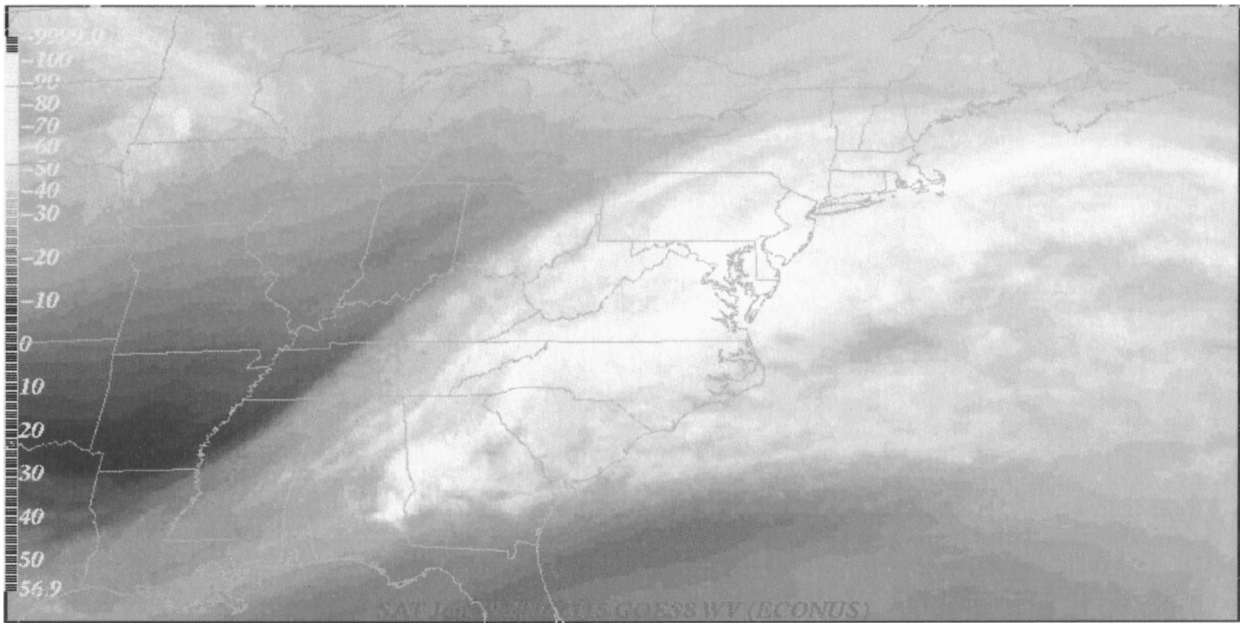

FIG. 12. *Geostationary Operational Environmental Satellite (GOES)-8* water vapor channel image at 2115 UTC 19 Jan 2002.

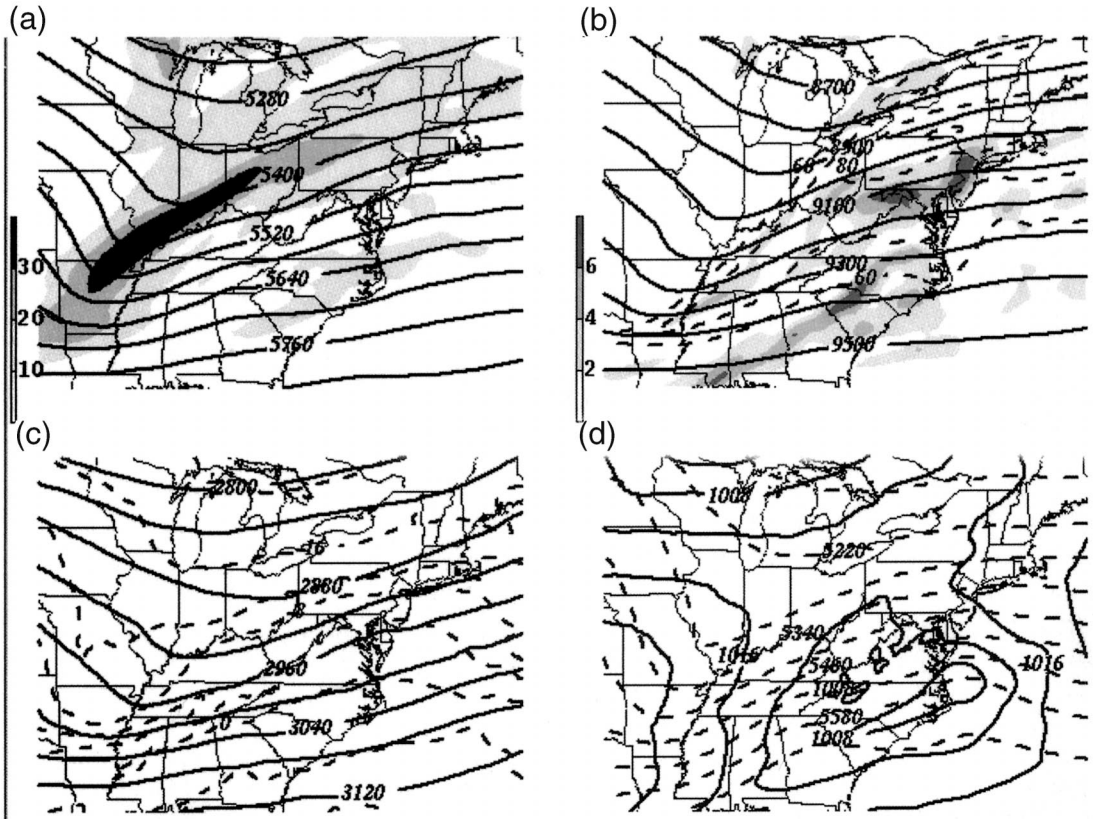

FIG. 13. Eta 9-h forecasts of (a) 500-hPa geopotential heights (m) and absolute vorticity (shaded, 10^{-5} s^{-1}), (b) 300-hPa geopotential height (m), isotachs (dashed, m s^{-1}), and divergence (shaded, 10^{-5} s^{-1}), (c) 700-hPa geopotential heights (m) and temperatures (dashed, °C), and (d) mean sea level pressure (hPa) and 1000–500-hPa thicknesses (dashed, m), all valid at 2100 UTC 19 Jan 2002.

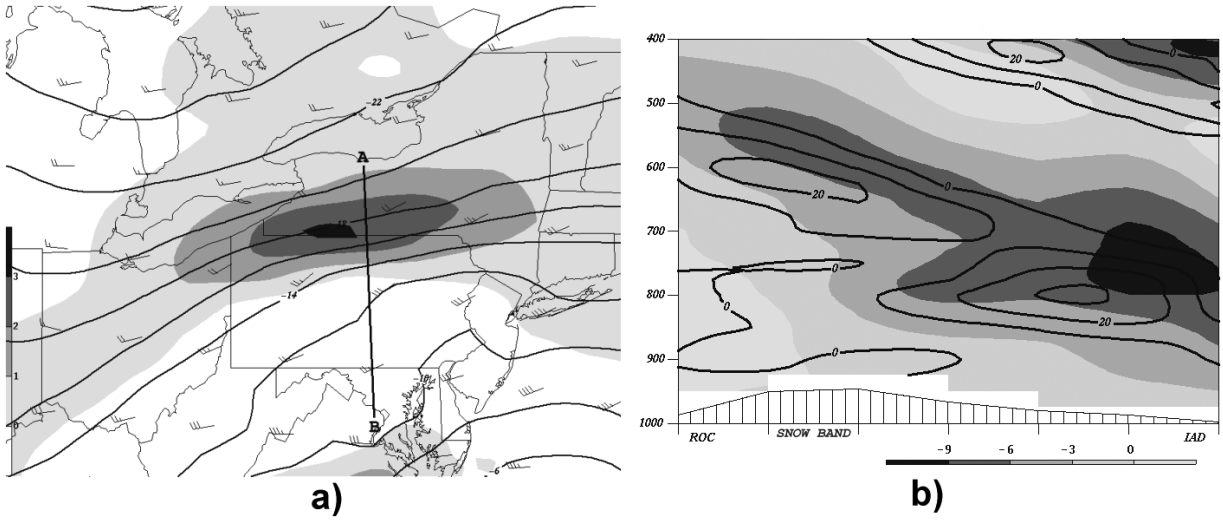

FIG. 14. (a) Eta 9-h 625-hPa frontogenesis [shaded, K (100 km)$^{-1}$ (3 h)$^{-1}$], winds (m s^{-1}), and temperatures (dashed, °C), valid for 2100 UTC 19 Jan 2002. (b) Eta cross section of frontogenesis [solid, 1×10^{1} K (100 km)$^{-1}$ (3 h)$^{-1}$] and omega [shaded, (μb s^{-1})], drawn from Rochester, NY (ROC, point A) to Washington, DC (IAD, point B), valid for the same time and date. The SNOW BAND caption refers to the approximate positioning of the heaviest snowfall along the *x* axis.

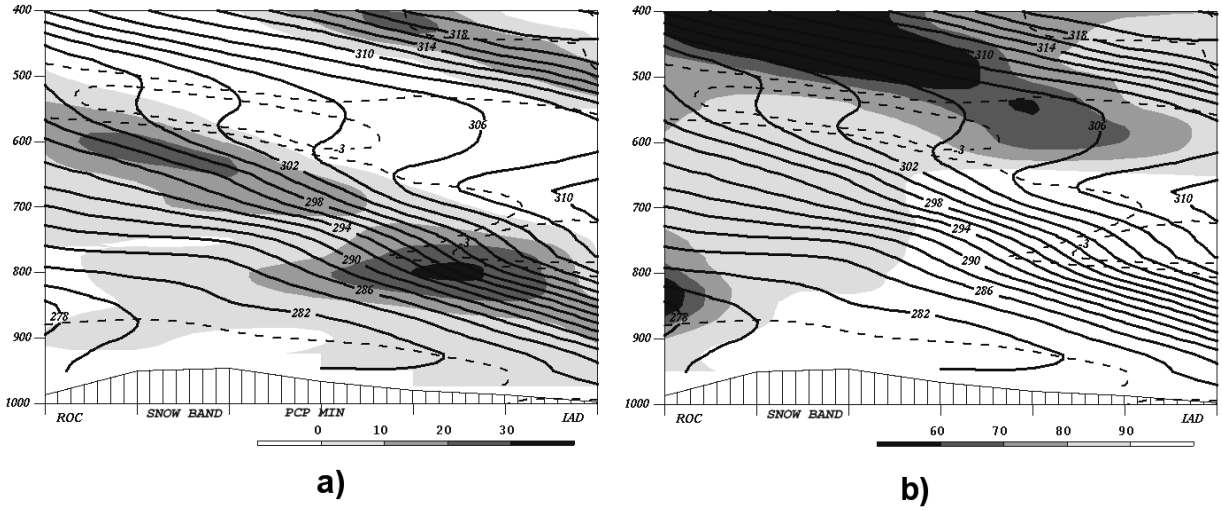

FIG. 15. (a) Eta cross section (same axis and valid time as Fig. 14b) of frontogenesis [shaded, K (100 km)$^{-1}$ (3 h)$^{-1}$], θ_e (solid, K), and negative EPV {dashed, [10^{-7} K (Pa s)$^{-1}$]}. SNOW BAND caption refers to the approximate positioning of the heaviest snowfall along the x axis. PCP MIN caption refers to the approximate positioning of the precipitation minimum along the x axis across central Pennsylvania. (b) Eta cross section (same axis and valid time as Fig. 15a) of θ_e (solid, K), negative EPV {dashed, [10^{-7} K (Pa s)$^{-1}$]}, and relative humidity (shaded, %). The SNOW BAND caption refers to the approximate positioning of the heaviest snowfall along the x axis.

positive θ_e advection below. In several documented cases, a link is made between differential θ_e advection and a pronounced midtropospheric dry slot associated with the main trough (Nicosia and Grumm 1999; DeVoir 1998). This dry slot typically rotates near or directly over the top of the lower-tropospheric CCB, acting to destabilize the column. For the 19 January case, however, differential θ_e advection resulted from the dry slot rotating over the top of a midtropospheric frontal boundary, as opposed to a lower-tropospheric CCB.

Another important aspect of this event was the microphysics of the precipitation. Figures 17a and 17b show the observed snow-to-liquid ratios and corresponding liquid equivalent amounts, respectively. Note the particularly high ratios that matched up quite well to the axis of the snowband (Figs. 9 and 10). Outside of cases that featured air masses of arctic origin (i.e., significant lake-effect snow or ''Alberta Clipper''–type systems), the majority of larger-scale snow events in the interior northeastern United States (including central New York) during the month of January have had observed snow-to-water ratios ranging from 11:1 to 17:1 (Doesken and Judson 1997). Based on this, the ratios that were observed on 19 January were quite out of the ordinary for the given time of year and location.

In order to investigate the reasons for the unusual snow-to-liquid ratios associated with this case, hourly Eta Model soundings were examined. Soundings from the analysis from 1200 UTC 19 January and the 9-h forecast valid at 2100 UTC are shown in Fig. 18. The sounding valid at 2100 UTC, which corresponded to the time of the heaviest snowfall, revealed several interesting features. Of particular note was a near-saturated layer about 2700 m in depth, with temperatures between −12° and −18°C, extending from about 850 to 600 hPa. Figure 18 shows that only a shallow layer (about 500 m in depth from near the surface to just above 900 hPa) existed where supercooled droplets and riming would be expected (temperatures between −5° and −10°C) at 2100 UTC. Given the presence of enhanced lift associated with the mesoscale band, along with the temperature and moisture profile at BGM described above, it is reasonably assumed that dendrites were the primary crystal type reaching the surface.

In order to better understand how the sounding profiles at BGM evolved leading up to and during the event, a time–height cross section of temperature advection and omega is shown (Fig. 19). At the time when the band was most intense (around 2100 UTC), a layer conducive to dendrite production extended from about 850 to 600 hPa (Fig. 18). In the lower part of this favorable dendrite zone (from around 825 to 700 hPa), the combined effects of evaporation, weak lift, and cold advection during the period from 1500 to 2100 UTC resulted in a cooling of the layer (Fig. 19). Meanwhile, the lower-tropospheric environment (from the surface to 850 hPa) experienced diurnal warming and weak warm advection. The net result was a steepening of the lapse rates in the surface to 700-hPa layer. In the upper part of the dendrite zone (700–600 hPa), more pronounced warm advection and upward motion occurred as a midtropospheric frontal zone developed over the region. The combined effects of strong, warm advection and moderate lift resulted in a slight warming of the 700–600-hPa layer. The combination of cooling in the 825–700-hPa layer and slight warming of the 700–600-hPa layer at BGM resulted in the creation of a deep isothermal layer near

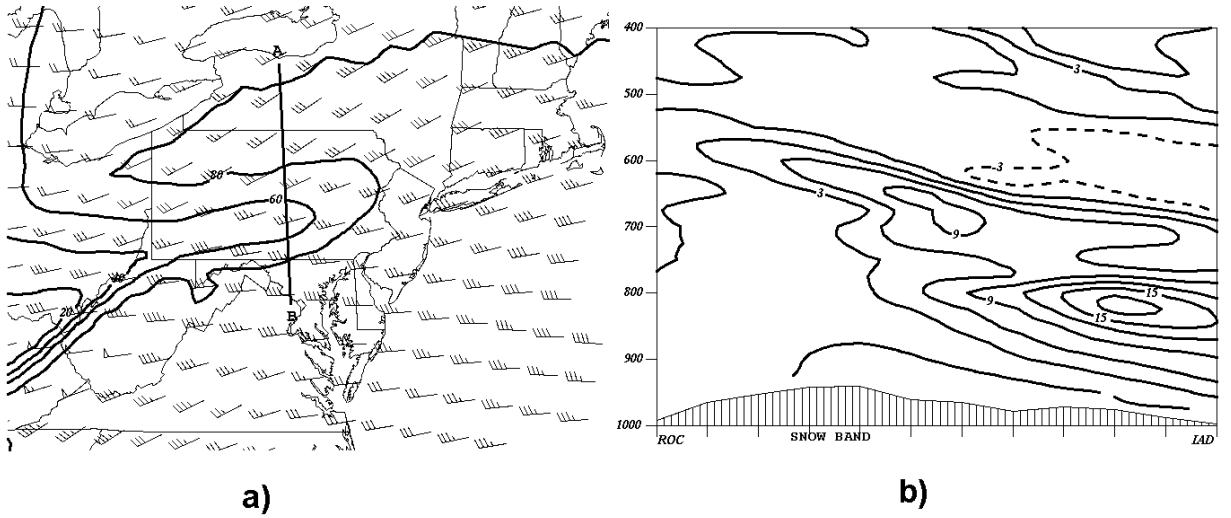

FIG. 16. (a) Eta 9-h 550-hPa relative humidity contours (%) and winds (m s^{-1}), valid at 2100 UTC 19 Jan 2002. (b) Eta cross section (same axis and valid time as Figs. 14b and 15) of θ_e advection [K 12 $h)^{-1}$]. The SNOW BAND caption refers to the approximate positioning of the heaviest snowfall along the x axis.

−15°C. Thus, the thermal structure of the atmosphere across southern New York developed to favor dendrites.

A final factor that likely led to the high snow-to-liquid ratios observed in this case was the light surface winds that were in place as the snow was falling. Surface winds observed at BGM during the peak of the storm were around 5 kt. It has been hypothesized that light surface winds are favorable for high snow-to-liquid ratios, because snow crystals that fall in light wind environments tend to remain intact when they land, allowing air pockets to develop between the crystals as they accumulate (Roebber et al. 2003; Gray and Male 1981). Conversely, crystals that fall with stronger surface winds tend to break up into smaller pieces, causing fewer air pockets to form.

In summary, the 19 January event appears to be an unusual case, particularly for the eastern United States, when several factors came together to produce an unexpectedly heavy snowfall. Most atypical was the lack of a deepening midtropospheric system and associated surface cyclone. Despite the absence of intense surface cyclogenesis, a band of heavy snow developed. This band formed near the northern edge of a dry slot, where destabilization from the differential θ_e advection narrowed and intensified the lift associated with a shallow region of midtropospheric frontogenesis. Unusually high snow-to-water ratios, which developed primarily due to the sustenance of a temperature profile that resulted in favorable precipitation microphysics, strongly aided accumulation efficiency in the most intense portion of the band.

5. Discussion

This paper compares and contrasts two banded, heavy snow events that occurred over New York and Pennsylvania in January 2002. The first case occurred on 6–7 January, and exhibited many classical characteristics of documented snowstorms with significant banding, while the second case, which occurred on 19 January, was more unusual.

Overall, the large-scale flow pattern was more amplified on 6–7 January, which led to stronger QG forcing (cf. Figs. 4 and 11). However, in both events, large-

TABLE 1. A comparison of surface observations from BGM and AVP in tabular format. The period of comparison is from approximately 1700 UTC 19 Jan 2002 to 0200 UTC 20 Jan 2002.

Observation time (UTC)	BGM	AVP
1653	2SM -SN, 21/17, 19005KT, SLP 191	5SM -SN, 23/19, 22005KT, SLP 193
1753	1/2SM SN, 21/19, 17008KT, SLP 176	4SM -SN, 24/20, 26004KT, SLP 177
1853	1/2SM SN, 21/19, 15005KT, SLP 156	2SM -SN, 23/21, 03004KT, SLP 152
1953	1/4SM SN, 21/19, 14005KT, SLP 152	3SM -SN, 24/21, 03004KT, SLP 148
2053	1/4SM SN, 20/19, 13004KT, SLP 148	2SM -SN, 24/21, 04006KT, SLP 141
2153	1/2SM SN, 20/19, 15004KT, SLP 146	2SM -SN, 25/21, 04004KT, SLP 139
2253	3/4SM -SN, 20/19, 12004KT, SLP 137	2SM -SN, 24/22, 07004KT, SLP 130
2353	1SM -SN, 20/19, 12004KT, SLP 125	1SM -SN, 24/21, 05005KT, SLP 115
0053	1SM -SN, 20/19, 10005KT, SLP 132	3/4SM -SN, 23/21, 02004KT, SLP 125
0153	3SM -SN, 20/19, 11004KT, SLP 122	3SM -SN, 23/21, 06005KT, SLP 109

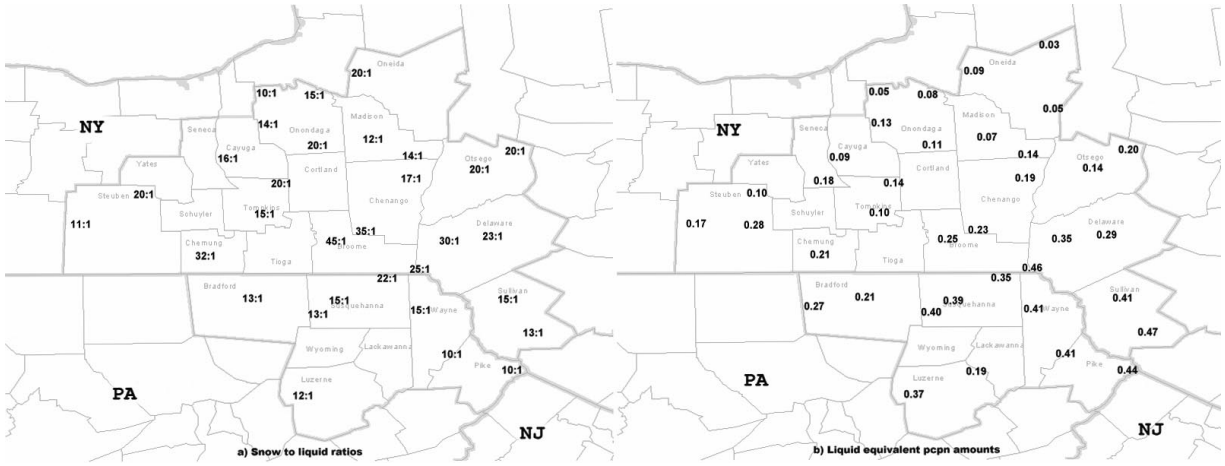

FIG. 17. (a) Observed snow-to-liquid ratios for precipitation that fell from 1200 UTC 19 Jan 2002 to 1200 UTC 20 Jan 2002. (b) Water equivalent precipitation totals for the same time frame (in.).

scale QG forcing was displaced from the strongest frontal scale forcing in the midtroposphere. On 6–7 January, the QG forcing was just to the south, while on 19 January it was further removed. Other studies have indicated that banding can occur within a wide range of circumstances regarding the separation between the QG and frontal scale forcing. For example, Banacos (2003) studied a few cases where intense banding occurred in areas where the frontal scale forcing was somewhat removed from larger-scale forcing, while Schumacher (2003) showed a case where heavy banding developed when upper-tropospheric QG forcing moved over a lower-tropospheric front.

In the two cases examined in this study the magnitude and horizontal extent of the frontogenesis appeared to be similar (Figs. 6a and 14a); however, the vertical extent of the frontal forcing was greater on 6–7 January, when the QG forcing was also stronger and closer to the frontal forcing (cf. Figs. 5 and 14b). The deeper frontogenesis on 6–7 January was also associated with larger values of upward vertical motion (omega) through a deeper layer. These observations imply that, while the frontal scale forcing supplied most of the intense lift in support of the heavy snowfall in these cases, the magnitude and location of the QG forcing also played a significant role by affecting the strength and depth of the frontal zone.

In both events, an elevated layer of reduced stability was present above the sloped frontal boundary. On 6–7 January, the environment appeared to be marginally and potentially unstable to slantwise ascent. Figure 7b portrays an atmosphere with neutral to weak midtropospheric PSI in the vicinity of the snowband, as indicated by total wind momentum surfaces that were nearly parallel to the θ_e contours. The flat nature of the momentum surfaces indicated that strong vertical wind

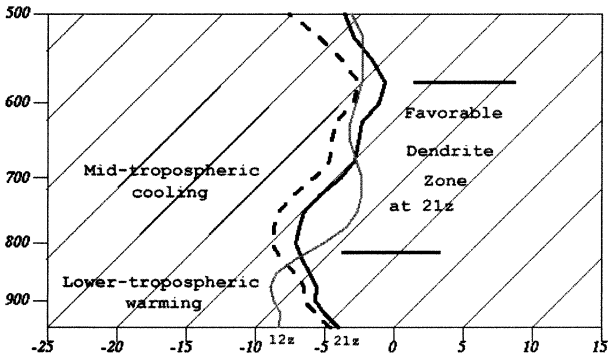

FIG. 18. Eta initial hour (solid gray, °C) vertical temperature profile, 9-h (solid black, °C) vertical temperature profile, and 9-h (black dashed, °C) vertical dewpoint temperature profile for BGM, valid at 1200 and 2100 UTC, respectively, 19 Jan 2002. Areas of warming and cooling between 1200 and 2100 UTC 19 Jan are indicated, along with areas favorable for dendritic snowflake production.

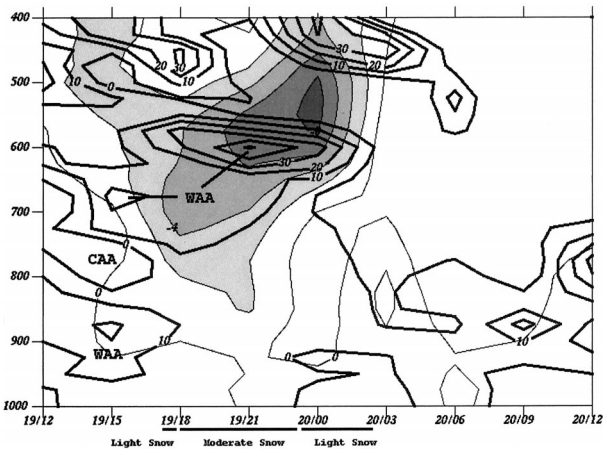

FIG. 19. An Eta time–height forecast of temperature advection [10^{-5} °C (s^{-1})] and omega (shaded, μb s^{-1}) at BGM from the 12 UTC 19 Jan model run. ''WAA'' indicates areas of warm advection and ''CAA'' indicates areas of cold advection. Observed weather at BGM is indicated at the bottom of the figure.

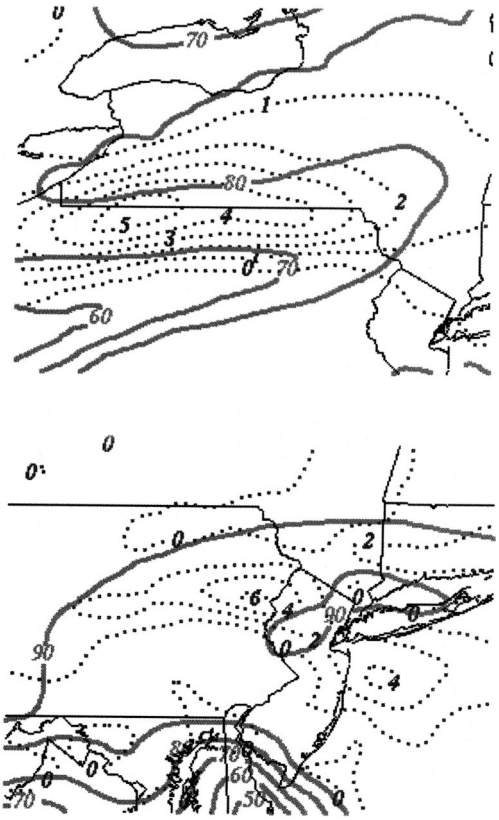

FIG. 20. Eta 500–700-hPa mean layer relative humidity (solid contours, %) and (top) 625-hPa frontogenesis {[K (100 km)$^{-1}$ (3 h)$^{-1}$], dotted} at 2100 UTC 19 Jan 2002 and (bottom) 600-hPa frontogenesis {[K (100 km)$^{-1}$ (3 h)$^{-1}$], dotted} at 0000 UTC 7 Jan 2002.

shear was present. By contrast, on 19 January the environment was characterized by PI. Figure 15b illustrates this by showing decreasing θ_e with height in the midtroposphere in a layer where the relative humidity decreased rapidly with height. Interestingly, there was no evidence for upright convection in this case, because visible satellite imagery (not shown) and WSR-88D data (Fig. 9) indicated that cellular convective elements did not exist within the broader snowband. Based on this, it seems likely that the PI was not released in the form of convection within the dry air above the front. However, the reduced stability likely did result in an enhanced frontal circulation and increased upward motion. It is theorized by the authors that the greater apparent instability on 19 January was the result of closer proximity between the elevated frontogenesis maximum and a midtropospheric dry slot (Fig. 20). As a result, lapse rates were steepened above the sloped frontal boundary by pronounced differential θ_e advection (Figs. 15a and 16b).

Prior work by Thorpe and Emanuel (1985), Knight and Hobbs (1988), Xu (1989), and Schultz and Schumacher (1999) shows that in an environment with strongly forced ascent underneath an area of negative MPV/EPV, intense multiple bands can develop within the upward branch of the frontal circulation. As mentioned above, the intensity and horizontal span of the frontogenesis for the cases being studied here were similar in magnitude. Considering this, it is interesting to note the different atmospheric responses for each event. Both cases featured bands of intense snowfall near the northern and western periphery of larger precipitation shields that were of relatively light intensity. On 6–7 January, several very narrow (about 10 km, as determined visually by the width of the 35-dB*Z* returns on WSR-88D mosaics) banded features accompanied a primary, more intense snowband that extended from central Pennsylvania into eastern New York (Fig. 1). Conversely, on 19 January, a single (about 30 km in width), less intense band was present across southern New York (Fig. 9). Results from studies cited earlier (Thorpe and Emanuel 1985; Knight and Hobbs 1988; Xu 1989) suggested that what determines whether single or multiple bands form does not depend on any single factor, but rather a balance of several. These include, most notably, the intensity and areal coverage of frontogenetic forcing, moisture availability, and the degree of negative EPV (Schultz and Schumacher 1999). In the cases studied in this paper, different blends of these factors elicited different atmospheric responses with respect to banded development (a very narrow, intense band, along with weaker multiple bands on 6–7 January, and then a single, broader band on 19 January). As a result, this observational study seems to substantiate the notion that the character of banded development is contingent upon a particular balance of frontal scale forcing, depth of moisture, and elevated instability.

Although each case exhibited intense snowfall rates associated with the banded features during their peak intensity [up to 2 in. h^{-1} (5 cm h^{-1}) on 19 January, and as much as 5 in. h^{-1} (12.5 cm h^{-1}) on 6–7 January], the role of the wind flow with respect to moisture advection and precipitation efficiency varied greatly. The lack of a midtropospheric dry slot near the frontal band on 6–7 January helped to maintain a greater depth of saturation through the layer of reduced stability above 700 hPa (Fig. 7). Also, stronger lower-tropospheric winds for this event likely provided a more robust inflow of Atlantic moisture into the frontal circulation. Meanwhile, on 19 January, the layer of saturation was relatively shallow due to the close proximity of the dry slot (Figs. 15b and 20). Also, with a relatively weak lower-tropospheric wind flow, it is likely that there was less moist inflow into the frontal circulation. For this event, the authors have theorized that the light wind flow contributed to a *lack* of significant thermal advection in the lower troposphere between 1800 UTC 19 January and 0000 UTC 20 January, which actually prolonged heavy snowfall by maintaining a favorable temperature structure in the vertical for dendrite production (Figs. 18 and 19) over a long time period. Stronger lower-tropospheric winds would likely have resulted in stronger warm advection, which may have adversely affected the thermal

profile by warming a portion of it above temperatures most favorable for dendrites to form. A shallower layer of preferred snowflake growth could have resulted in more typical snow-to-water ratios and lower accumulation efficiencies.

Finally, it should be noted that the weak large-scale forcing associated with the 19 January case does not necessarily conflict with results from Novak et al. (2004), which indicated that strong large-scale forcing and intense lower-tropospheric cyclogenesis is needed for significant snowbanding. They used strict criteria for selecting their cases, including a specification that at least 25.4 mm of liquid precipitation or 12.5 mm of liquid equivalent precipitation must occur with an event to warrant its inclusion in their study. Based on such criteria, the event on 19 January would not have qualified for acceptance into their database, because the maximum observed liquid equivalent amount with the event was just 12 mm.

6. Summary

The two cases presented here demonstrate that banded, heavy snow can occur within a wide variety of large-scale flow patterns. Although much research to date has concentrated on cases with intense QG forcing, its absence does not necessarily preclude the occurrence of banded, heavy precipitation. The common factors appear to be the collocation of frontogenesis with reduced stability. However, it is shown in this study that banded snowstorms come in a variety of shapes and sizes, which are modulated not only by the large-scale flow pattern, but by frontal scale, and even microscale, factors. For example, in our study, while both cases exhibited banding, the characteristics of such differed. The first case, associated with narrow, intense banding, was characterized by strong QG forcing located just south of the snowband, deep frontogenesis, pronounced lift, and deep saturation. The second case, associated with a less intense, broader band, featured weaker QG forcing further removed from the snowband, shallower frontogenesis, weaker lift, and a smaller saturated layer.

Both cases illustrate well the perils of trying to assess banding potential by simply viewing model fields in plan view (Wetzel and Martin 2001). This was especially true on 19 January, when the frontogenetical circulation and concurrent instability existed within shallow vertical layers, respectively. Thus, it is recommended that operational forecasters make use of cross sections to identify layers of interest, rather than rely solely on analysis of standard data levels. Whenever it appears that frontogenetic forcing could be significant and potentially produce banded precipitation, viewing a cross section of frontogenesis, EPV (or MPV), omega, and relative humidity would assist forecasters in establishing a linkage between frontal scale forcing, instability, and upward motion. Looking at streamlines of the ageostrophic wind component in a cross section could also help to visualize the three-dimensional structure of a given frontal circulation. In addition, model soundings have great utility in determining the microphysical state of the atmosphere and its potential effect on accumulation efficiency for a given time and location.

Acknowledgments. The authors would like to thank the work of three anonymous reviewers, whose suggestions and comments greatly improved this manuscript. We would also like to thank Dave Novak, Jeff Waldstreicher, and Heather Hauser at the NWS Eastern Region Headquarters for helpful reviews of the paper, as well as helpful comments and suggestions while the research was being done. The authors would also like to thank Phil Schumacher (NWS FSD), Dave Schultz [University of Oklahoma and National Severe Storms Laboratory (NSSL)], and John Nielson-Gammon (Texas A&M University) for helpful comments during the research and writing phases of the project. We would also like to thank Ron Murphy, the Information Technology Officer at NWS BGM, for help with some of the figures, and Liz Page and Dolores Kiessling (COMET) for providing us with much of the data necessary for the project. Finally, we would like to thank Bob Rozumalski (COMET) and Steve Chiswell (National Institute for Water and Atmosphere Research, New Zealand) for information on using GEMPAK to calculate **Q**-vector divergence, and to Jon Vanausdall, for installing the latest version of GEMPAK locally for use in the study.

REFERENCES

Banacos, P. C., 2003: Short range prediction of banded precipitation associated with deformation and frontogenetic forcing. Preprints, *10th Conf. on Mesoscale Processes,* Portland, OR, Amer. Meteor. Soc., CD-ROM, P1.7.

Bennetts, D. A., and B. J. Hoskins, 1979: Conditional symmetric instability—A possible explanation of frontal rain bands. *Quart. J. Roy. Meteor. Soc.,* **105,** 945–962.

Black, T. L., 1994: The new NMC mesoscale model: Description and forecast examples. *Wea. Forecasting,* **9,** 265–278.

Bluestein, H. B., 1993: *Synoptic-Dynamic Meteorology in Midlatitudes.* Vol. II, *Observations and Theory of Weather Systems.* Oxford University Press, 594 pp.

Carlson, T. N., 1980: Airflow through midlatitude cyclones and the comma cloud pattern. *Mon. Wea. Rev.,* **108,** 1498–1509.

Clark, J. H. E., R. P. James, and R. H. Grumm, 2002: A reexamination of the mechanisms responsible for banded precipitation. *Mon. Wea. Rev.,* **130,** 3074–3086.

desJardins, M. L., K. F. Brill, S. Jacobs, S. S. Schotz, and P. Bruehl, 1992: GEMPAK5 users manual version 5.1. NASA GSFC, National Meteorological Center, Unidata Program Center/UCAR, 267 pp.

DeVoir, G. A., 1998: Conditional symmetric instability—Methods of operational diagnosis and case study of 23–24 February 1994 eastern Washington/Oregon snowstorm. National Weather Service Western Region Tech. Memo 254, 16 pp.

Doesken, N. J., and A. Judson, 1997: *The Snow Booklet, A Guide to the Science, Climatology, and Measurement of Snow in the United States.* Department of Atmospheric Science, Colorado State University, 86 pp.

Gray, D. M., and D. H. Male, 1981: *Handbook of Snow Principles: Processes, Management and Use.* Pergamon Press, 776 pp.

Gray, S. L., and A. J. Thorpe, 2001: Parcel theory in three dimensions and the calculation of SCAPE. *Mon. Wea. Rev.*, **129,** 1656–1672.

Knight, D. J., and P. V. Hobbs, 1988: The mesoscale and microscale structure and organization of clouds and precipitation in midlatitude cyclones. Part XV: A numerical modeling study of frontogenesis and cold-frontal rainbands. *J. Atmos. Sci.*, **45,** 915–931.

Kocin, P. J., and L. W. Ucellini, 1990: *Snowstorms along the Northeastern Coast of the United States: 1995–1985. Meteor. Monogr.*, No. 44, Amer. Meteor. Soc., 280 pp.

Martin, J. E., 1998a: The structure and evolution of a continental winter cyclone. Part I: Frontal structure and the occlusion process. *Mon. Wea. Rev.*, **126,** 303–328.

——, 1998b: The structure and evolution of a continental winter cyclone. Part II: Frontal forcing of an extreme snow event. *Mon. Wea. Rev.*, **126,** 329–348.

——, J. D. Locatelli, and P. V. Hobbs, 1992: Organization and structure of clouds and precipitation on the mid-Atlantic coast of the United States. Part V: The role of an upper-level front in the generation of a rainband. *J. Atmos. Sci.*, **49,** 1293–1303.

Miller, J. E., 1948: On the concept of frontogenesis. *J. Meteor.*, **5,** 169–171.

Moore, J. T., and T. E. Lambert, 1993: The use of potential vorticity to diagnose regions of conditional symmetric instability. *Wea. Forecasting*, **8,** 301–308.

Nicosia, D. J., and R. H. Grumm, 1999: Mesoscale band formation in three major northeastern United States snowstorms. *Wea. Forecasting*, **14,** 346–368.

Novak, D. R., L. F. Bosart, D. Keyser, and J. S. Waldstreicher, 2002: A climatological and composite study of cold season banded precipitation in the northeast United States. Preprints, *19th Conf. on Weather Analysis and Forecasting*, San Antonio, TX, Amer. Meteor. Soc., CD-ROM, P6.5.

——, ——, ——, and ——, 2004: An observational study of cold season–banded precipitation in northeast U.S. cyclones. *Wea. Forecasting*, **19:** 993–1010.

O'Handley, C., and L. F. Bosart, 1989: Subsynoptic structure in a major synoptic scale cyclone. *Mon. Wea. Rev.*, **117,** 607–630.

Power, B. A., P. W. Summers, and J. d'Auignon, 1964: Snow crystal forms and riming effects as related to snowfall density and general storm conditions. *J. Atmos. Sci.*, **21,** 300–305.

Roebber, P. J., S. L. Bruening, D. M. Schultz, and J. V. Cortinas Jr., 2003: Improving snowfall forecasting by diagnosing snow density. *Wea. Forecasting*, **18,** 264–287.

Sanders, F., 1986: Frontogenesis and symmetric stability in a major New England snowstorm. *Mon. Wea. Rev.*, **114,** 1847–1862.

Schultz, D. M., and P. N. Schumacher, 1999: The use and misuse of conditional symmetric instability. *Mon. Wea. Rev.*, **127,** 2709–2732; Corrigendum, **128,** 1573.

Schumacher, P. N., 2003: An example of forecasting mesoscale bands in an operational environment. Preprints, *10th Conf. on Mesoscale Processes*, Portland, OR, Amer. Meteor. Soc., CD-ROM, P8.1.

Skerritt, D. A., R. W. Przybylinski, and R. A. Wolf, 2002: A study on the 6 December 1995 Midwest snow event: Synoptic and mesoscale aspects. *Natl. Wea. Dig.*, **26,** 52–62.

Thorpe, A. J., and K. A. Emmanuel, 1985: Frontogenesis in the presence of small stability to slantwise convection. *J. Atmos. Sci.*, **42,** 1809–1824.

Weismueller, J. L., and S. M. Zubrick, 1998: Evaluation and application of conditional symmetric instability, equivalent potential vorticity, and frontogenetic forcing in an operational forecast environment. *Wea. Forecasting*, **13,** 84–101.

Wetzel, S. W., and J. E. Martin, 2001: An operational ingredients-based methodology for forecasting midlatitude winter season precipitation. *Wea. Forecasting*, **16,** 156–167.

Xu, G., 1989: Extended Sawyer–Eliassen equation for frontal circulations in the presence of small viscous moist symmetric stability. *J. Atmos. Sci.*, **46,** 2671–2683.